# Mechanical Design Considerations for Taiwan Photon Source

J.R. Chen*, J.C. Chang, H.C. Ho, G.Y. Hsiung, C.K. Kuan, Z.D.Tsai, T.C.Tseng and D.J. Wang
National Synchrotron Radiation Research Center
101 Hsin-ann Road, Hsinchu Science Park, Hsinchu, 30076 Taiwan
* also at Department of Biomedical Engineering and Environmental Sciences,
National Tsing-Hua University, Hsinchu, 30013 Taiwan

*Abstract*

*A three Gev synchrotron light source, Taiwan Photon Source (TPS), is proposed at the National Synchrotron Radiation Research Center (NSRRC). In its preliminary design, the TPS has a circumference of 518.4m with 24 long straight sections and a low emittance of 1.7nm-rad. The mechanical issues, such as vibration, survey and alignment, precision mechanics, temperature stability, high heat load absorber, and so on, are essential to the TPS performance. This study presents the design considerations and some preliminary designs for the major mechanical subsystems or components of the TPS.*

## 1. Introduction

Due to its capability to produce brilliant lights with wide spectrum range, from infra-red to hard x-rays, third generation synchrotron light sources attract growing numbers of studies on basic and applied research. To produce hard x-rays, three large machines, a 6 GeV machine at ESRF, a 7 GeV machine at APS and an 8 GeV machine at SPring-8, were constructed in 1990s. Medium energy (~3 GeV) machines recently have become the mainstream, and several synchrotron light sources are being constructed or commissioned around the world. [1]

At the NSRRC, the 1.5 GeV synchrotron light source (Taiwan Light Source, TLS), has been operated for 13 years since being dedicated in 1993. The performance of the TLS has markedly improved in the fields of mechanical stability, electrical stability, feedback system and superconducting technologies. The top-up injection mode recently was successfully applied to TLS. Although the superconducting wigglers at the TLS increase the photon energy to the hard x-ray range, the intensity and brightness of the photon beam at TLS lag far behind the advanced facilities, including both those currently in operation and those being planned. To fulfil user demand for hard x-ray, a 3 GeV synchrotron light source, the Taiwan Photon Source (TPS), was proposed at the NSRRC. The TPS is a very stable machine, and aims to achieve high brightness of $10^{21}$ p/s/0.1%bw/mm$^2$/mrad$^2$ (at 10 keV) by using advanced insertion devices. [2]

The basic performance, stability and reliability are the key concerns in designing a synchrotron light source. From the mechanical engineering perspective, system aspects such as dimension and tolerance, ground stability (both settlement and vibration), temperature stability, dynamic performance (such as frequency domain and time constant of response) of the system, gas flow, material, heat transfer etc., require careful design. The following sections depict and discuss the mechanical design considerations for the TPS.

## 2. The TPS

In its preliminary design, the TPS has a circumference of 518.4m with 24 long straights and features low emittance of 1.7nm-rad [2]. Super conducting radiofrequency (rf) cavities, top-up mode injection, stable mechanical system and powerful feedback system are equipped with TPS to achieve enhanced performance. Advanced insertion devices (ID), such as in-vacuum undulator, elliptical polarized

undulator and superconducting undulator, are installed to offer high brightness photons. Owing to limitations of space at the NSRRC site and to save costs in booster building and accessory utilities, a concentric booster located at the same tunnel as the storage is designed. Figure 1 illustrates a 3-D layout of a section of the TPS. Moreover, Fig. 2 illustrates the curves of the photon beam brightness of the TPS and the other light sources for comparison. Table I lists the preliminary TPS parameters.

Fig. 1 A 3-D layout of a section of the TPS.

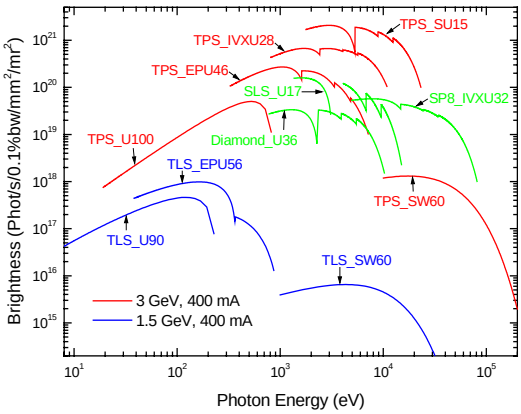


Fig.2 Curves of the photon beam brightness of the TPS, and of the other light sources for comparison.

Stringent specifications are followed in designing the mechanical system at TPS. For advanced experiments, a stable photon beam with intensity fluctuation of < 0.1% is required. A value of < 10% in the fluctuation of the electron beam orbit and size is generally set as an index accordingly. [3] In the real case, the requirements can be much more stringent than the above value, because of several potential sources that can contribute to the photon beam instability.

*Table I Main machine parameters of the TPS.*

| **Parameter** | **TPS** |
|---|---|
| Lattice Energy (GeV) | 3.0 - 3.3 |
| Current (mA) | 400 (300@3.3GeV) |
| Circumference (m) | 518.4 |
| No. of Long Straights | 24 |
| Emittance (nm-rad) | 1.7 |
| Bending Radius (m) | 7.257 |
| Bending field (T) | 1.38 |
| RF Frequency (MHz) | 500 |

## 3. Settlement and Vibration

### *3.1 Ground settlement and vibration*

The existing plateau at the present site of the NSRRC is too small to accommodate the TPS. Concerning the ground stability, a site with same altitude will be prepared so that the slab of the TPS building can sit on a grade with good quality. No piles or empty structures exist underneath the TPS slab. The results of the TLS building and surrounding areas revealed average ground settlement of < 50 μm per year over the 10 years of operations of the TLS, with larger settlement occurring during the first two years. The

above number thus is set as a specification of the ground settlement to the TSP. The long term stability at the TLS implies that the stability in the ground settlement of the TPS could maintain a similar result provided stringent civil construction standards are followed.

On the other hand, the ground vibrations at the NSRRC site are not as stable as at some other synchrotron light sources [4]. Figure 3 illustrates the result of the power spectrum density (PSD) measured at the NSRRC site. A peak at ~3Hz was measured in the PSD curve. It was shown by comparing the differences between the working hours and rest hours that the daily traffic and cultural activities are the major vibration source at low frequencies, The integrated value from 4Hz to 100Hz was ~ 40nm in the vertical direction. The measurements at the boarder of the NSRRC, by the main traffic roads, showed an even higher amplitude of ~ 80nm. Civil engineering approaches, such as increasing the stiffness of the slab and using isolation methods, are considered for reducing the ground vibrations associated with outside activities. However, it is difficult to accurately forecast the damping (or amplification) factor that the civil engineering can contribute to ground vibration. A design goal of < 40nm integrated from 4 to 100 Hz for application to the ground vibration after the completion of the slab of the TPS tunnel.

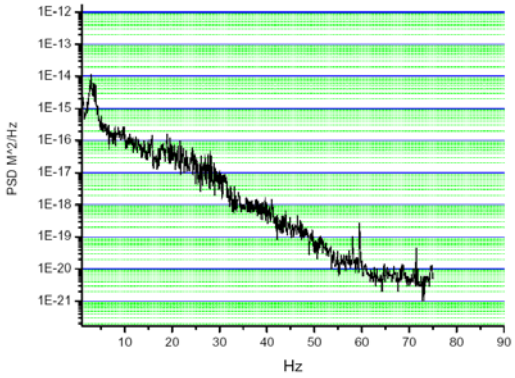


Fig.3 Typical ground vibration PSD curve at NSRRC.

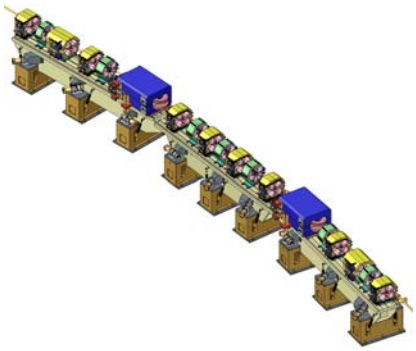

Fig.4 A 3-D layout of MGA design for TPS.

### *3.2 Magnet girder assembly and alignment*

Besides civil construction, magnet girder assembly (MGA) crucially impacts the effects of ground settlement and vibration on beam stability. The MGA could even create resonance and amplify the vibration. Reduce the magnification factor, from ground vibration to the magnet, is always a major goal in MGA design.

Figure 4 shows a 3-D layout of the preliminary MGA design for the TPS. An MGA comprises four main parts, including the magnets, girder, cam mover and pedestal. Conventional electromagnetic magnets are used for the dipole-, quadrupole- and the sextupole magnets. Laminated low-carbon steel sheets provide the base material of the magnet yoke. Trim coils are wound on the sextupoles as correctors and skew-quadrupoles.

The magnets are precisely fixed to the girder by matching the pre-machined reference planes at both the bottom of the magnets and the top of the girder. The alignment error of all the magnets at the same girder is < 30 μm. Given this stringent requirement, the amplification factor of the quadrupole displacement to the beam orbit distortion can be reduced by approximately five times. [2] The results of the girder prototype demonstrated that the number can be reached given careful control of the machining process. Regarding the alignment between two neighbour girders, position sensors with a precision of micron meters are located at the interface of the two girders. The alignment error among three girders at the same cell of the lattice is estimated to be < 50 μm using this method.

To adjust the girders to accuracies of micrometers, a remote-controlled mover system is designed at the TPS. Not only is the resolution of the adjustment better than that for manual adjustment, but the adjustment requires much less time. This remote controlled system enables the girders of the machine to easily be readjusted in the event of big disturbances, such as earthquakes, while also being maintained at better values the rest of the time.

Regarding the potential degradation of the stiffness of the girder system by introducing the mover system, a primary eigen frequency of > 30 Hz is set as a basic design criterion for the TPS girder. The mover is an eccentric cam system incorporating six point-contact ball-transfer-units. An expanded 3-groove kinematic mounting system, supported at six locations, increases the system stability. Figure 5 depicts the measurements of the natural frequency of the girder system (without magnet). The results revealed that the first eigen frequencies of the girder system (without magnets) are 43 Hz and 45 Hz in the horizontal and vertical directions, respectively. Figure 6 shows the transfer function of the girder (floor to magnet), when magnets are positioned on it. The first two eigen frequencies are 23/32 Hz and 35/39 Hz in the horizontal and vertical directions, respectively. The peaks at 23 Hz (horizontal) and 35 Hz (vertical) in Fig.6 are small and may not indicate the girder characteristics. To increase the first resonance frequency above 30 Hz, a detailed study of the peak of 23 Hz and a method of locking the girder following alignment are being performed. A damping-rods system is designed at the TPS girder to reduce the amplification of the ground vibration to the magnet.

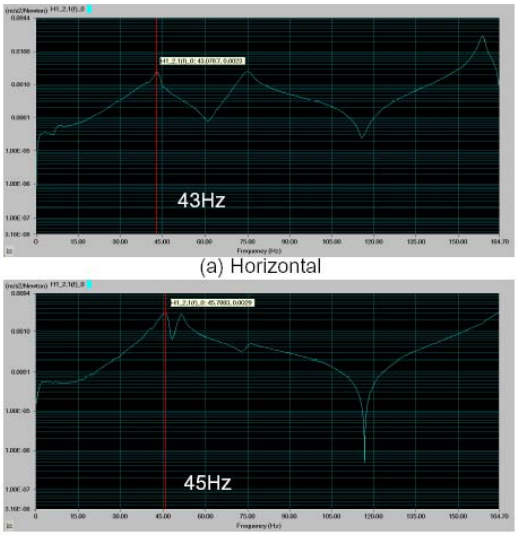


Fig.5 Natural frequency of MGA (w/o magnet).

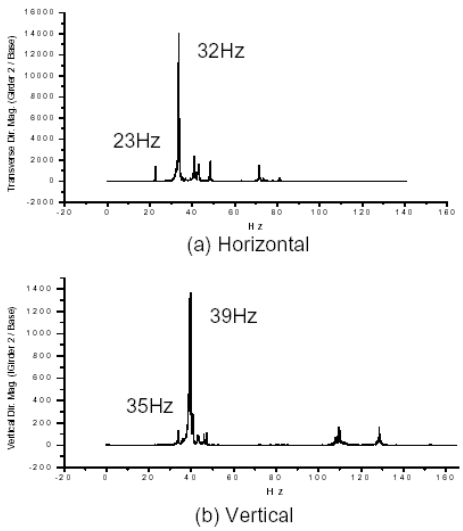


Fig.6 Transfer function of MGA (floor to magnet).

## 4. Temperature Stability

Among the influences on subsystem performance and beam stability, thermal effect is the most critical in the low frequency domain. From the results of the TLS [5], the sensitivity of beam orbit or beam size to the temperature fluctuation could reach up to tens microns per degree C. To achieve beam stability of sub-microns, concerning the amplification factor from the displacement in magnets to the beam orbit (about 10-50), the tolerance of temperature fluctuation for a component with typical dimensions (ten centimetres to meters) and thermal expansion coefficient (in the order of 10ppm/˚C) should be <0.1 ˚C or better.

In relation to thermal effect, the primary concern is to prevent structural thermal deformation, followed by controlling thermal stability of thermal sources. Selecting a material with a small coefficient of thermal expansion, using isolating materials and increasing the heat capacity of the material are possible means of suppressing thermal deformation. Three aspects of control of thermal sources include water

temperature, air-conditioning, and dissipation of heat from electric power. The TPS design devotes considerable attention to these issues. The design target of cooling water and ambient air is controlled to within a range of 0.1°C.

The water temperature stability, from the cooling tower water, chilled water to the de-ionized (DI) water supplied to the devices, is controlled step-by-step. The requirements are ±0.5°C, ±0.2°C, and ±0.1°C for the cooling tower water, chilled water and DI water, respectively. Varied frequency inverters are used to stabilize the flow rate under varying load. Careful designs in the piping arrangement (primarily for the capacity requirement from the related devices) and the resolution and linearity of valve control are also required to achieve a stable temperature. For certain highly sensitive devices, a temperature stability of ±0.01°C is required; a buffer tank with enough capacity is fitted in the loop of the DI water. A compact tank with mixing mechanism is to be used for special component. [6]

Notably, in many light sources the air temperature fluctuation severely influences the beam stability. Unlike the cooling water system, which is a closed loop system, the air system is partially open. For example, it is difficult to avoid air exchange between the circulating air and the outdoor fresh air or exchange between two neighbouring environments with different temperature conditions. Since the dissipation of thermal energy into the air is difficult to control, most devices use cooling water for heat removal, and the power supplies for the accelerator are arranged in air-conditioned rooms.

Both the stability over time and the spatial uniformity must be considered in air temperature control. A tiny difference in temperature distribution can cause severe buckling of large components such as the girder and the insertion device. Stable temperature control in chilled water and hot water has to be reached before a stable control in the air temperature. Under the condition of stable water temperature, the air temperature stabilization system controls the percentage water flow rate (chilled water and hot water). Uniform air temperature is achieved by adjusting the direction of the nozzles at the air outlets. A simulation was conducted for the TPS storage ring tunnel, and the results indicated a stable and uniform temperature distribution. [7]

Given variation of the line voltage or operating conditions in the accelerator, temperature variation occurs in the devices. The most notable examples are the ramping up and down in strength of the magnets when the electron beam is injected and the decay of the strength of the electron beam over time. Since these two issues negatively impact the stability of the accelerator, TPS uses a full energy injector and a top-up injection to reduce the influence. The top-up mode can also help maintain the stability of the optical devices in the photon beam lines.

## 5. Vacuum Chamber, Pressure and Thermal Load

Besides the displacements resulting from vibration and temperature fluctuation, the residual gas in the beam duct and the rf impedance of the chamber wall influences the beam stability. The vacuum system of a synchrotron light source plays two primary roles, reducing and removing the gas and heat generated by the synchrotron light on the chamber wall (or component), maintaining a clean environment for the circulating beam and preventing component failure. Although these two issues appear different in principle, the two sources share the same origin, namely irradiation from synchrotron light. Sometimes the solutions for the two issues conflict with one another, and thus trade offs must be assessed. On the other hand, regarding the rf impedance of the chamber wall, the structure of the beam duct must also be considered in the vacuum system design.

### *5.1 Pumping configuration and vacuum pressure*

Because of its high thermal conductivity, easy machining, light weight and low outgassing rate, aluminium alloy is selected as the vacuum chamber material for the TPS. Two types of pumping

configurations exist, distributed pumping and localized pumping, which are applicable to the environment of the synchrotron light source. Both pumping configurations are adopted at the TPS.

The ante-chamber and localized pumping configuration are designed for the TPS bending-chambers (B-chamber). Figure 7 schematically depicts the TPS B-chamber. The B-chamber is fabricated using NC machining with ethyl alcohol as a lubricant to ensure that the cleanliness of the chamber surface. An automatic welder is designed for the large-size B-chamber to achieve labour and cost savings. To minimize the photoelectric yield, and thus the gas desoption yield, the incident angle of the photon beam on the wall is set to ~ 90 degrees. The long B-chamber is designed to increase the percentage of synchrotron light confined inside the bending chamber, which reaches approximately 93%. Because the B-chamber of the TPS has a length of 4 to 5m, three to four pumps can be installed and more design options, for example differential pumping structure, can be implemented to reduce the local pressure.

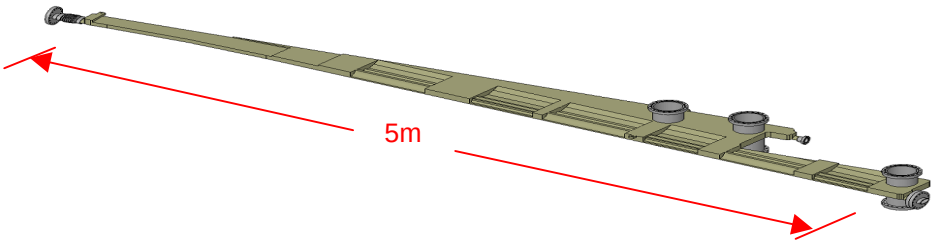


Fig.7 A 3D schematics of the TPS B-chamber.

ID-chambers in the straight section are made by extrusion. Distributed pumping using NEG strips is used for the ID-chambers, where the conductance and space for the pumps are highly limited. Because the beam channel is too narrow to be coated with getter material, a non-evaporable getter (NEG) strip is selected for the distributed pumping in the ID-chamber. The NEG strip is installed in a side-channel along the beam duct. [8] This arrangement can reduce the potential for the NEG powders to be dropped into the beam channel where they will destroy the circulating beam. Frequent installation of the IDs in a third-generation synchrotron light source such as the TPS is inevitable. However, the vacuum pressure is severely degraded following ID installation. Concerning the slower beam dose accumulation in the ID-chamber compared to the B-chamber, most of the ID-chambers must be fabricated and installed before the TPS is commissioned. The ID-chambers that are unavailable at the time of commissioning of the TPS will be cleaned in a photon beam line before installation.

The advantage of the TPS B-chamber (ante-chamber, normal incident) is that it reduces the desorption yield and large-size to accommodate effective localized pumping, as shown in Table II, which illustrates the PSD- related parameters of the TLS and TPS. Notably, the table shows that the outgassing rate per cell (which has a length of ~ 20 m for both ring), Q, of the TPS is identical to that of

*Table II: The PSD-related parameters of TPS.*

| ***Parameter*** | ***TLS*** | ***TPS*** | ***Remark*** |
|---|---|---|---|
| *Beam energy (GeV)* | *1.5* | *3.0* | |
| *Beam current (mA)* | *200* | *400* | |
| *Q per cell (Torr*l/s), at η= 1x10$^{-5}$ molec./e* | *~1x10$^{-6}$* | *~1x10$^{-6}$* | *same* |
| *Beam duct material* | *Aluminum* | *Aluminum* | |
| *Bending angle of dipole magnet (deg.)* | *20* | *7.5* | |
| *Percentage of synchrotron light in B-chamber* | *77%* | *92.8%* | *more* |
| *Nominal pumping speed (per cell)* | *~ 4000 L/s* | *~ 4000 L/s* | *same* |
| *Pump ports per cell* | *13 (on axis)* | *10 (off axis)* | *less* |
| *Pressure increase at η= 1x10$^{-5}$ molec./ e* | *~1.3nTorr* | *~ 0.3nTorr* | *1/4* |

the TLS. However, the average pressure of the TPS is just a quarter of that of the TLS, primarily because of the more gas desorptions and pumping speeds being localized at the B-chamber. Additionally, there is a lower requirement for the pumping port at the TPS and it can be located at the offset of the beam channel, so that a better rf impedance can be achieved. The following designs support an average pressure of ~$3x10^{-10}$ Torr, at a high desorption rate of $1x10^{-5}$ molecules/electron. [9]

### *5.2 High heat load absorber*

The beam energy of the TPS is not as high as that of a high-energy machine with an energy range of > 6 GeV, so the thermal problem is less severe at the TPS. Nevertheless, the thermal load of the synchrotron light on the aluminum B-chamber of the TPS will be unacceptably high if the irradiated wall is a short distance from the source point. An independent copper absorber is typically employed to protect the crotch of a B-chamber. The design is complex because the space is limited and an independent crotch absorber must be integrated. The aluminum chamber is a good absorber if the heat load is not excessive . Increasing the distance from the source point effectively reduces the thermal load on the chamber wall. A larger B-chamber not only has a lower thermal density, but also has a lower pressure, as stated in the preceding section. The "crotch" of the TPS B-chamber is designed under such considerations.

Considering the smallest photo-desorption rate, the incident angle at which the synchrotron light hits the chamber wall is ~ 90 degree. The maximum power density on the chamber surface is ~22 W/$mm^2$ (400mA at 3GeV). Improving the geometries of the cooling channel (fins cut into the end wall of the chamber) and the stepped surface (0.4mm height x 2mm depth, Fig. 8), enabled the maximum temperature of the chamber surface to be held at ~109°C (~138°C at the maximum capacity 350mA at 3.3 GeV of the TPS), which is tolerable for aluminum. Meanwhile, a flange port is available for an independent copper absorber, which is to be installed when the beam energy or current is increased.

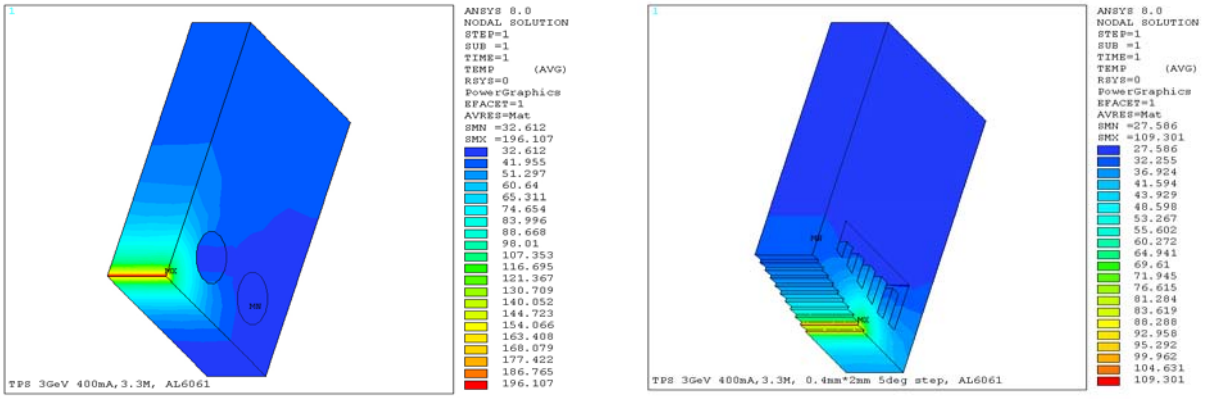


(a) (b)

Fig.8 Before (a) and after (b) using stepped surfaces and fins in the cooling channel enables the maximum temperature of the aluminum chamber surface to be reduced from ~196°C to ~109°C.

The radiation power from the insertion devices could exceed that from the bending magnet. Most of the power from these devices is to be treated at the front end. Table III presents the parameters of the IDs of the TPS. A photon beam is incident at a grazing angle on an independent copper absorber with a long surface. Thermal power will be received by absorbers at various stages, including the pre-mask, mask, photon shutters and slits.

*Table III The parameters of the IDs of TPS.*

| | U100 | EPU70 | SW60 | EPU60 | EPU46 | IVX U28 | SEPU25 | SU15 |
|---|---|---|---|---|---|---|---|---|
| Photon Energy (keV) | 0.02-0.9 | 0.07-4 | 2-100 | 0.12-5 | 0.4-6 | 1-12 | 0.7-10 | 3-25 |
| Current (mA) | 400 | 400 | 400 | 400 | 400 | 400 | 400 | 400 |
| $\lambda$(mm) | 100 | 70 | 60 | 60 | 46 | 28 | 25 | 15 |
| $N_{period}$ | 45 | 64 | 33 | 75 | 98 | 160 | 80 | 600 |
| By (Bx) (T) | 1.0 | 1.0 (0.77) | 3.5 | 0.9 (0.7) | 0.76 (0.49) | 0.9 | 1.2 (0.58) | 1.5 |
| $K_{max}$ | 14.2 | 6.4 (1.7) | 19.6 | 5.04 (3.92) | 2.79 (1.07) | 2.35 | 2.78 (1.35) | 2.1 |
| L (m) | 4.5 | 4.5 | 2 | 4.5 | 4.5 | 4.5 | 2 | 9 |
| Gap (mm) | 15 | 15 | 17 | 15 | 15 | 7 | 5 | 5 |
| Peak Power Density ($kW/mr^2$) | 24.7 | 29 | 52.5 | 30.6 | 33.3 | 64.2 | 43.1 | 88.6 |
| Total Power (kW) | 16.5 | 11.7 | 62.4 | 9.3 | 6.6 | 9.3 | 7.3 | 11.4 |
| Type | Hybrid | Pure | SC | Pure | Pure | Hybrid | SC | SC |

### *5.3 Structure of the vacuum chamber and component*

Impedance is an important issue in vacuum chamber design. The impedance is associated with the discontinuities in the beam duct structure, such as at the ports for pumps and diagnostic instruments, long slots for synchrotron light extraction, flange gaps, valves, bellows, the transition piece and the chamber wall itself.

The nominal interior cross section of the TPS beam duct is an ellipse with axial lengths of 32mm x70mm. The special components, such as rf cavities, ID chambers and the ceramic chambers for injection, are designed with different cross sections. Transition pieces of sufficient length are used to change the cross section from a nominal cross section smoothly to a different one. The mismatch in lining up two neighbor chambers should be maintained at < 0.5mm. In the ID chamber, furthermore, the gap is narrow so the impedance problem becomes more severe. In a superconducting ID, the narrow gap of the ID-chamber can cause problematic heating of the low-temperature components. A chamber with high conductivity is advantageous. Like heating caused by beam impedance, the shining of synchrotron light on the small-gap ID chamber can also cause a problem. A special design that protects the chamber wall from the synchrotron light, especially in the vertical direction, will be very valuable.

As stated in the preceding section, most of the pumping ports of the TPS are offset from the beam channel, reducing the discontinuities at the beam channel, resulting in a better rf impedance. At TPS, the corrugated structure of the bellows, the gap between two flanges and the cavity structure inside the sector gate valves are all shielded to make a smooth beam channel. Any protrusion associated with such arrangement is < 0.5mm.

## 6. Summary

The mechanical issues that arise in the construction of a synchrotron light source are of wide interest. The main mechanical design considerations, described herein, are related to ground settlement and vibration, magnet girder assembly, temperature stability, the vacuum chamber structure and the high heat load absorber for the TPS. An environment with very stable vibration, air temperature and water temperature must be provided. A temperature fluctuation of < 0.1°C for both air and water, a vibration

amplitude of < 40nm (integrated from 4 to 100 Hz) and an alignment error of < 30μm on the MGA, are required to maintain a stable beam with sub-micron variation in both orbit and size. The preceding sections of this work presents some simulation and test results for the TPS design.

Like factors that cause displacement or instability in the dimensions or position of the major components, the structure of the vacuum chamber also affects the performance of the circulating beam. At TPS, the B-chamber is designed with a length of 4-5m, so the heat density on the chamber wall associated with the synchrotron light at normal incidence is acceptable. A large B-chamber also benefits the design in reducing vacuum pressure by the arrangements of localized pumping and normal incidence of synchrotron light (to reduce the photo-desorption yield). For an ID, an independent copper absorber with a photon beam at a grazing incidence on the long absorber surface is adopted. Thermal power is removed by different absorbers, like the pre-mask, the mask, the photon shutters, slits and other components at various stages.

The discontinuity in the cross section of the beam duct of the TPS is eliminated by careful design of the components. The discontinuities in the beam duct cross section are steps of < 0.5mm or better. Shielding pieces are employed to reduce the rf impedance of some components with corrugated or cavity structures.

## 7. Acknowledgement

The authors would like to thank their colleagues of the Light Source Division and the Instrumentation Development Division of the NSRRC for their efforts in designing the TPS.

## 8. References

1. The papers in the proceedings of Shanghai Symposium on Intermediate-Energy Light Sources, the 25th ICFA Advanced Beam Dynamics Workshop, Shanghai, Sep. 24-26, 2001.
2. "Taiwan Photon Source- Proposal of Conceptual Design (Draft Ver.1)," NSRRC report, April 2006.
3. R. Hettel, "Beam Stability at Light Sources," SRI 2001, Madison, USA, Aug 22, 2001.
4. Proceedings of the 22nd Advanced ICFA Beam Dynamics Workshop on Ground Motion in Future Acclerators, SLAC, Stanford, USA, Nov. 6-9, 2000.
5. J. R. Chen, D. J. Wang, Z. D. Tsai, C. K. Kuan, S. C. Ho, and J. C. Chang, *"Mechanical Stability Studies at the Taiwan Light Source",* MEDSI 2002, ANL, Argonne, USA, Sep. 5-6 (2002).
6. Z.D. Tsai, J.C. Chang, C.Y. Liu and J.R. Chen, "*High Precision Temperature Control and Analysis of RF Deionized Cooling Water System*," Proc. PAC2005, Knoxville, USA, May 12-16, 2005.
7. J.C. Chang et. al, this proceedings.
8. G.Y. Hsiung, D.J. Wang, J.G. Shyy, S.N. Hsu, K.M. Hsiao, M.C. Lin, and J.R. Chen, "*Installation of a 14 mm Vacuum Chamber for an Undulator in the 1.3 GeV Storage Ring at Synchrotron Radiation Research Center*", J. Vac. Sci. & Technol. A15(3), 723-727 (1997).
9. J.R. Chen, G.Y. Hsiung, C.K. Chan, T.L. Yang, C.K. Kuan, S.N. Hsu, C.C. Chang , C.Y. Yang, H.P. Hsueh and C.L. Chen, "*Vacuum System Developments at the National Synchrotron Radiation Research Center - from the 1.5 GeV TLS to the 3.3 GeV TPS*," to be published in J. of the Vacuum Society of Japan.